Virchows Archiv A Pathol Anat (1989) 415:357–366

Virchows Archiv A
Pathological Anatomy and Histopathology

An immunohistochemical study of the fibrosing process in paraquat lung injury

Hiroki Hara[1,2], Toshiaki Manabe[2], and Takuji Hayashi[3]

[1] Department of Medicine, and
[2] Department of Human Pathology, Kawasaki Medical School, 577 Matsushima, Kurashiki, Okayama 701-01, Japan
[3] Department of Pathology, Kuakini Medical Center, Honolulu, Hawaii, USA

Summary. Twenty-nine autopsy cases of paraquat-induced lung injury were studied by histological and immunohistochemical methods. Two stages of injury were identified. In the early stage, the alveolar epithelium degenerates but the epithelial basement membrane remains intact. In the late stage, the epithelial basement membrane is focally disrupted, the mesenchymal cells grow into the alveolar space, and intra-alveolar fibrosis appears. In spite of these pathological changes, the original framework of the alveolar wall is preserved in many areas. Intra-alveolar fibrosis may follow as a consequence of damage to the epithelium without severe damage to the underlying basement membrane, which occurs at the stage of organization. Morphological variants of intra-alveolar fibrosis seem to occur not only to the size of the defect of the basement membrane but also to the difference in the stages of evolution at the time the lesion is studied. The epithelium regenerates along the basement membrane in the early stage of re-epithelialization, but grows over the luminal aspect of intra-alveolar fibrous tissue which has been laid on the remaining basement membrane in the late stage. It is speculated that the regeneration of epithelial cells may develop without any association with the basement membrane when a fibrous tissue covers the original basement membrane.

Key words: Paraquat poisoning – Pulmonary fibrosis – Immunohistochemistry

Introduction

Pulmonary fibrosis occurs in a variety of conditions and may progress to an end stage ("honeycomb lung"). Whatever the mechanism, the patterns of pulmonary fibrosis can be classified into two morphological categories, interstitial and intra-alveolar (Katzenstein and Askin 1982b; Basset et al. 1984; Fukuda et al. 1987). The latter type may also play an important role in the pathogenesis of interstitial fibrotic lung diseases. In fact, it has been reported that interstitial lung diseases are much more frequently associated with intra-alveolar fibrosis than hitherto thought (Basset et al. 1986).

Paraquat (1,1′-dimethyl-4,4′-bipyridium dichloride), one of the most widely used herbicides in Japan, causes severe and often fatal pulmonary disorders in the human when ingested. In Japan, paraquat is usually ingested during attempted suicide. Intra-alveolar fibrosis is one of the characteristic pathological features in the late stages of paraquat lung in addition to interstitial fibrosis (Copland et al. 1974; Spencer 1985). Due to the relative ease of determining the interval between the ingestion and the time of initial examination, many clinical (Copland et al. 1974; Rebello and Mason 1978; Dearden et al. 1978; Mukada et al. 1978; Parkinson 1980; Yamaguchi et al. 1986; Moriya et al. 1988; Hara et al. 1988) and experimental studies of the paraquat lung (Smith and Heath 1973; Thurlbeck and Thurlbeck 1976; Sykes et al. 1977; Greenberg et al. 1978; Schoenberger et al. 1984; Skillrud and Martin 1984; Fukuda et al. 1985) have been reported.

Paraquat lung reveals morphological evidence of acute alveolar injury characterized by inflammatory cell infiltration, haemorrhage, and oedema, followed by a hypercellular "proliferative" phase with loss of the alveolar structures and intra-alveolar and interstitial fibrosis (Copland et al. 1974; Rebello and Mason 1978; Parkinson 1980). It is generally stated that diffuse injury of alveolar epithelium and disruption of the epithelial basement

Offprint requests to: H. Hara

membrane are prerequisites for the initiation of intra-alveolar fibrosis (Basset et al. 1986; Fukuda et al. 1987) and similar processes may take place in the paraquat lung. Accurate identification of the alveolar epithelium, epithelial basement membrane and mesenchymal cells taking part in the process is essential for better understanding of the pathological mechanisms of intra-alveolar fibrosis. The identification of these elements by routine light microscopy is, however, difficult. Electron microscopy has high resolving power but is of limited value in the examination of large areas. Immunohistochemical techniques have been employed in the study of lung injury but results are still inconclusive.

This communication describes the histological and immunohistochemical findings of the lungs in 29 autopsy cases of paraquat poisoning. An attempt was made to reconstruct the sequence of the fibrosing process. Tissue responses vary among the patients who differed in age, sex, the amount of paraquat ingested, treatments and other factors. Therefore, the sequence of events we have reconstructed is unlikely to be a completely accurate presentation. However, our observations are supported by a considerable amount of compiled information, and allow us to consider the sequence of events leading to pulmonary fibrosis.

Materials and methods

In the past 6 years (1981–1987), 29 autopsies of paraquat poisoning were performed at the Department of Pathology, Kawasaki Medical School Hospital. The patients were comprised of 16 males and 13 females, aged 20–82 years of age (mean age, 48 years). Gramoxone (24% paraquat) was ingested orally in 26 of 29 patients, by inhalation in one patient, by intramuscular injection in one patient, and by an unknown route in one patient. Paraquat intoxication was confirmed in 25 cases by sodium dithionite test on urine. The estimated amounts of ingested paraquat ranged from 4 to 375 ml. However, the amounts did not accurately reflect the actual amounts absorbed because of emesis and/or gastric lavage. The treatments included early gastric or intestinal lavage, and charcoal column haemoperfusion or haemodialysis was also performed in all cases, except for case 7. Oxygen therapy and assisted ventilation were administered in all cases of respiratory failure. The survival time after paraquat ingestion ranged from 8 h to 24 days.

The lungs obtained from the patients with paraquat intoxication were fixed by instillation of 10% buffered formalin solution via airways. Tissue blocks from selected areas were routinely processed and embedded in paraffin. Four μm thick sections were stained with haemotoxylin and eosin (H&E), Masson trichrome, elastic-van Gieson (EVG), periodic acid-methenamine silver (PAM) stain, and Pap's silver impregnation. Controls were obtained from grossly normal areas of the lungs resected for cancer. The control specimens were processed and stained in the same manner.

The following antibodies were used in the immunohistochemical study; anti-collagen type IV and anti-laminin antibodies for the detection of the basement membrane; anti-epithelial membrane antigen (EMA) antibody, anti-factor VIII-related antigen antibody, anti-vimentin antibody, and anti-desmin antibody for alveolar epithelial cells, endothelial cells, mesenchymal cells and cells with myoid differentiation respectively.

Four μm thick sections were deparaffinized in xylene, dehydrated in alcohol, washed in distilled water, and then rinsed in Tris-buffered saline (TBS, pH 7.6). All sections were treated with 0.07% trypsin (1:250 Trypsin, DIFCO, Detroit, MI) and 0.1% $CaCl_2$, pH 7.8, at 37° C for 5 to 20 min to unmask antigenic sites (Huang et al. 1976; Ordóñez et al. 1988). After washing distilled water, the tissue sections were treated with 1% hydrogen peroxide in methanol for 20 min to inhibit endogenous peroxidase activity. Subsequently, the sections were washed with distilled water, rinsed in TBS, and incubated with normal swine serum at a dilution of 1:20 in TBS for 20 min to block nonspecific antibody reactions.

The sections were then incubated for 30 min with primary antibodies: mouse monoclonal anti-human collagen type IV antibody (BioGenex Laboratories, Dubrin, CA; 1:2,000), mouse monoclonal anti-human laminin antibody (Behring Diagnostic, La Jolla, CA; 1:1,000), mouse monoclonal anti-human EMA antibody (DAKO, Santa Barbara, CA; 1:50), mouse monoclonal anti-human factor VIII-related antigen antibody (DAKO; 1:100), mouse monoclonal anti-human vimentin antibody (DAKO; 1:200), and mouse monoclonal antihuman desmin antibody (DAKO; 1:100).

After washing with TBS, the sections were incubated with peroxidase-labelled rabbit anti-mouse IgG (DAKO) for 30 min at a dilution of 1:50. Then they were washed with TBS, and further incubated with peroxidase-labelled swine anti-rabbit IgG (DAKO) for 30 min at a dilution of 1:50 or 1:100. Washed with TBS again, the sections were reacted in a solution of 0.06% 3,3′-diaminobenzidine tetrahydrochloride (DAB) (Sigma, St. Louis, MO) and 0.03% hydrogen peroxide in TBS for 4 to 9 min. They were washed with water, counterstained with Gill's haematoxylin, dehydrated, and mounted. All procedures were carried out at room temperature except for the steps of trypsinization. The positive, negative and substitution controls were stained in parallel with the test materials.

In order to differentiate alveolar macrophages from fibroblasts, some sections were also stained by PAP method (Sternberger et al. 1970), applying rabbit anti-human lysozyme antibody (1:400), and rabbit anti-human alpha-1 antitrypsin antibody (1:500). Some sections derived from the late stages of paraquat lung were double-stained with anti-collagen type IV antibody and anti-EMA antibody by a double immunoenzymatic method with DAB and 3-amino-9-ethylcarbazole (AEC) as a chromogen, respectively, in order to elucidate the relationship between the basement membrane and the regenerating epithelium. For this purpose, we followed the procedure of Chen et al. (1987).

Formalin pigment in some sections was removed with saturated alcoholic picric acid before staining by the immunoperoxidase (IP) method (McGovern and Crocker 1986).

Results

Histopathological features of 29 cases are summarized in Table 1 and have been reported elsewhere (Moriya et al. 1988). The different sections of the same case showed marked variation in each pathological feature.

The histological changes of the lungs of the

Table 1. Histopathological features

Case no.	Survival time	Oedema	Haemorrhage	Hyaline membrane	Interstitial fibrosis	Intra-alveolar fibrosis	Enlargement of alveolar ducts
1	8 h	+	−	−	−	−	±
2	9	−	−	−	−	−	−
3	12	−	−	−	−	−	−
4	20	+	+	±	−	−	−
5	22	++	+	±	−	−	−
6	23	±	+	−	−	−	−
7	26	+	±	−	−	−	−
8	34	++	+	±	−	−	−
9	49	++	+	±	−	−	−
10	52	++	±	±	−	−	±
11	73	++	±	+	−	−	−
12	90	+	−	+	−	−	−
13*	93	−	−	−	−	−	−
14	108	++	+	±	−	−	−
15	7 days	++	++	+	+	+	±
16	7	+++	++	+	+	+	−
17	7	+++	++	+	+	+	±
18	8	++	+++	++	++	+	+
19	9	++	++	+	+	+	++
20	11	++	+++	++	++	+	+
21	12	++	+++	++	++	+	+
22	13	++	+	+	++	++	++
23	14	++	++	+	+++	++	+
24	14	++	++	+	++	++	++
25	14	++	++	+	+++	+++	+
26	15	++	++	+	++	++	++
27	20	++	++	++	++	+++	++
28	20	++	+++	+	+++	+++	++
29	24	++	++	+	+++	+++	+

Code: −, none; ±, equivocal; +, few or slight; ++, some or moderate; +++, many or marked;

* Case 13 died due to sepsis without respiratory failure

patients who expired within 12 h after the ingestion of paraquat, were subtle and hardly observable in H&E sections. By 20 h after ingestion, congestion, oedema, haemorrhage, and infiltration by neutrophils and macrophages became apparent in various degrees. Progressive haemorrhage was noted in the alveolar spaces and reached a maximum on the 8th day. Exudative changes with inflammatory cell infiltration were present in all cases after 20 h except for case 13, and became prominent on the 7th day. They were first localized along the alveolar ducts. Intra-alveolar fibrosis first appeared on the 7th day in the form of incorporation of exudates and cell debris on the mural aspect, and later in the form of filling in the lumen of alveoli, alveolar ducts, and respiratory as well as terminal bronchioles. On occasion, intra-alveolar fibrosis consisted of three layers over the original alveolar structures; loose fibrous tissue, hyaline membrane, and loose connective tissue with haemorrhage (Fig. 1). On the 13th day and thereafter, the air spaces became obliterated by young loose connective tissue. The original framework could be clearly identified in the EVG-stained sections (Fig. 2) and PAM-stained sections. Intraluminal connective tissue was usually loose and hypocellular. This finding was most evident in Masson trichrome sections. Intraluminal polypoid fibrous tissue (Masson bodies) were also observed in the cases from day 20 and 24.

The interstitium was oedematous particularly after the 2nd day. Interstitial fibrosis appeared on the 7th day and became prominent by the 11th day.

The immunohistochemical findings were as follows. Alveolar and bronchiolar epithelial cells were identified by means of immunostaining with anti-EMA antibody. Both type I and II pneumocytes were positively stained. The immunoreactivity of alveolar epithelium was well preserved for 12 h after ingestion. After 20 h, however, the immunoreactivity gradually decreased and completely disappeared from 52 h until 7 days, except in 2 cases. In all cases, however, bronchiolar epitheli-

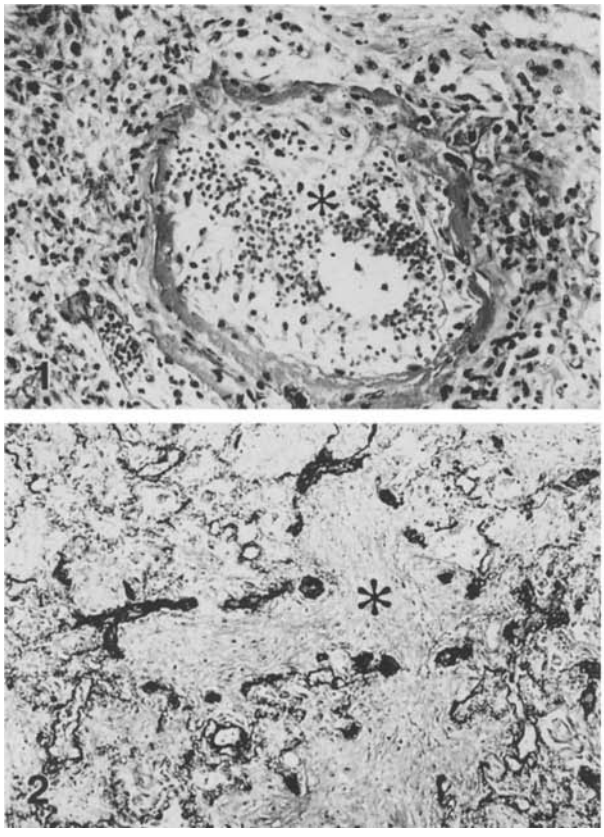

Fig. 1. Case 28. Note the formation of hyaline membrane between the alveolar walls and intra-alveolar loose fibrous tissue. They may be caused by oxygen administrated afterward. *Asterisk* shows alveolar lumen. (H&E, ×150)

Fig. 2. Case 29. Alveolar and bronchiolar lumens (*asterisk*) are completely obliterated with fibrous tissue. (EVG, ×60)

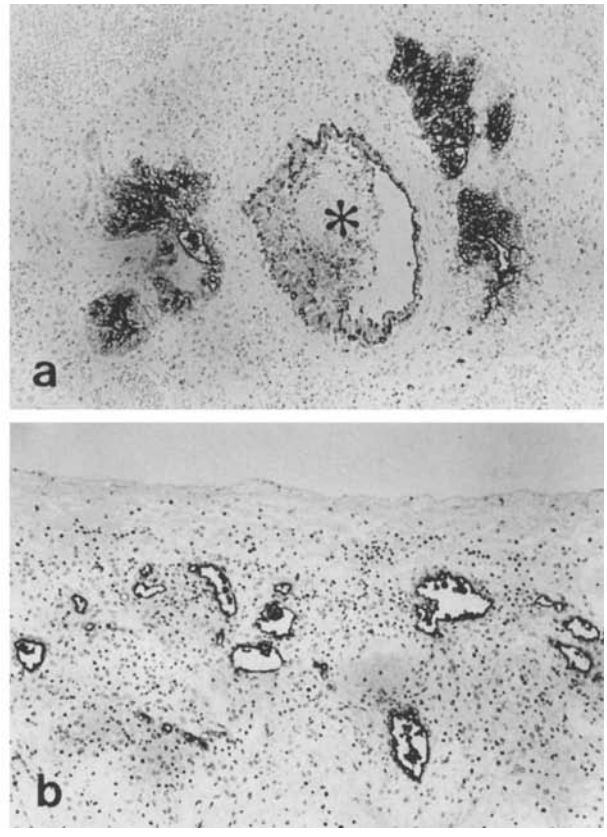

Fig. 3. Case 25. EMA-positive cells are present in the peribronchiolar (**a**) as well as subpleural area (**b**). *Asterisk* shows bronchiolar lumen. (IP-haematoxylin for EMA, a: ×70, b: ×70)

um continued to stain with anti-EMA antibody. On the 8th day and thereafter, immunoreactive cells reappeared in the focal areas along the thickened alveolar walls. They appeared to be regenerating epithelial cells. On the 14th day, these immunoreactive cells were distributed only in the peribronchiolar and subpleural areas (Figs. 3a and b). The immunoreactive cells were cuboidal in shape, closely apposed to each other and lined along the thickened alveolar walls, giving an appearance of follicular pattern (Fig. 4). The double staining for collagen type IV and EMA clearly demonstrated that the regenerating epithelial cells were arranged along the persisting basement membrane on the 14th day and that fibrous tissue intervened between the regenerating epithelial cells along the luminal border and the remaining vascular and epithelial basement membranes on the 24th day (Fig. 5).

Anti-collagen type IV antibody demonstrated the basement membrane of alveolar and bronchiolar epithelium, vascular endothelium, the schwannian cells of the nerves, and smooth muscle cells of the bronchi of the control specimens. The basement membrane of the endothelium was stained more strongly than that of the alveolar epithelium and showed a homogeneous and linear pattern along the alveolar wall. Two distinct immunoreactive layers of the basement membrane could be distinguished in some areas of the alveolar walls, representing the epithelial and endothelial basement membranes.

In 28 of 29 paraquat lung cases, there was strong immunoreactivity for collagen type IV, even in the cases with loss or degeneration of the overlying alveolar epithelial cells and no EMA immunoreactivity. The alveolar and vascular basement membranes were clearly separated in the cases of interstitial oedema (Fig. 6). The epithelial basement membrane was irregular, fragmented and indistinct in the areas of inflammatory cell infiltra-

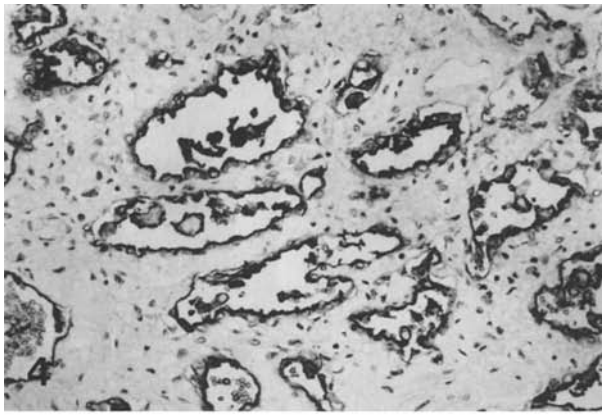

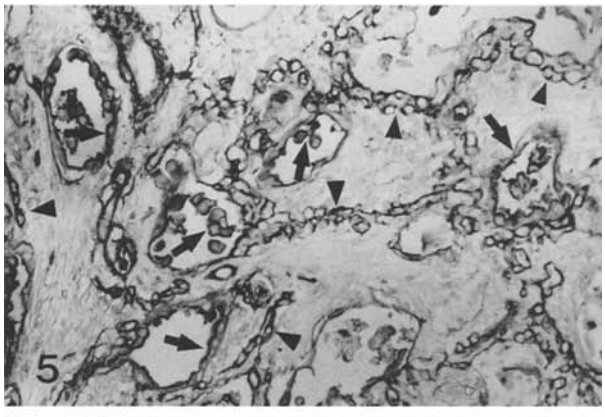

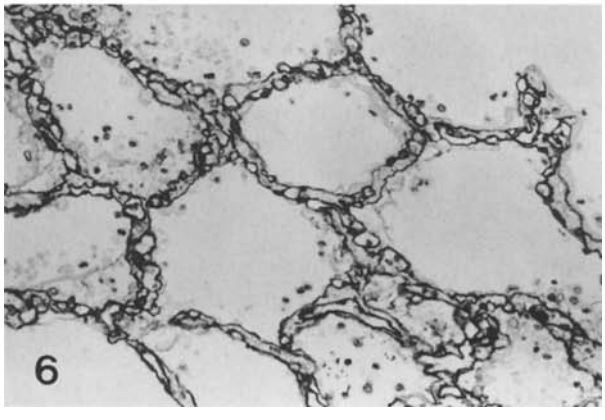

Fig. 4. EMA-positive cuboidal cells assume follicular arrangement in case 29. (IP-haematoxylin for EMA, ×170)

Fig. 5. Case 29. EMA-positive regenerating cells (*arrows*) are arranged along the luminal surface of intraalveolar fibrous tissue away from the collagen type IV-positive original epithelial basement membrane (*arrowheads*). Note that in this black-and-white photomicrograph, collagen type IV, which was stained brown in the original material appears slightly darker than EMA, which was red in the original. (IP double staining for EMA and collagen type IV without counterstain, ×150)

Fig. 6. Case 20. Reaction for collagen type IV shows the separation of the basement membrane of the alveolar epithelia and capillary endothelia in the case of interstitial edema. (IP-haematoxylin for collagen type IV. ×150)

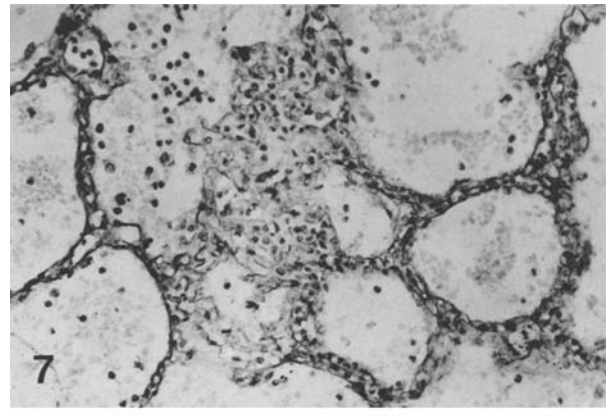

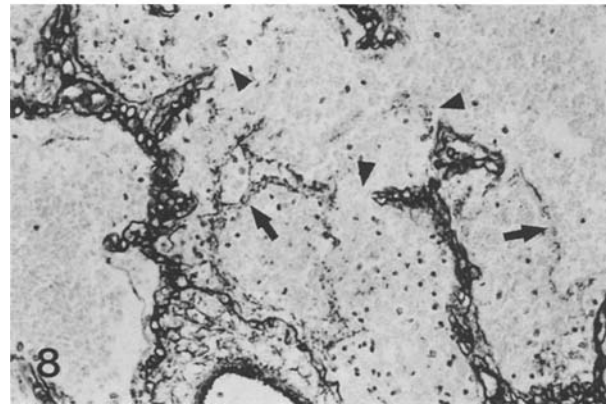

Fig. 7. Case 15. Staining pattern of collagen type IV is irregular and indistinct in the area of inflammation. (IP-haematoxylin for collagen type IV, ×150)

Fig. 8. Case 18. The basement membrane is disintegrated (*arrows*) and disrupted (*arrowheads*) in some areas. (IP-haematoxylin for collagen type IV, ×150)

tion (Fig. 7). In the areas where the underlying lung tissue was disintegrated or disrupted, the immunoreactive granular substance was noted in the alveolar lumen (Fig. 8). In the cases of intra-alveolar fibrosis (Fig. 9a), the capillary basement membranes were well preserved in most areas whereas the epithelial basement membranes were focally disrupted (Fig. 9b). In the cases of what appeared to be interstitial fibrosis in the H&E sections, collagen type IV was well preserved, thereby leaving the original framework intact. Thus the fibrous tissue was in fact intra-alveolar, leaving some residual alveolar spaces empty (Fig. 10). The immunoreactivity was absent adjacent to the abscess.

The staining patterns of laminin were similar to those of collagen type IV. The staining by laminin was, however, faint and sometimes almost indistinguishable from the background staining.

Factor VIII-related antigen used as a marker of endothelial cells was demonstrated only in the

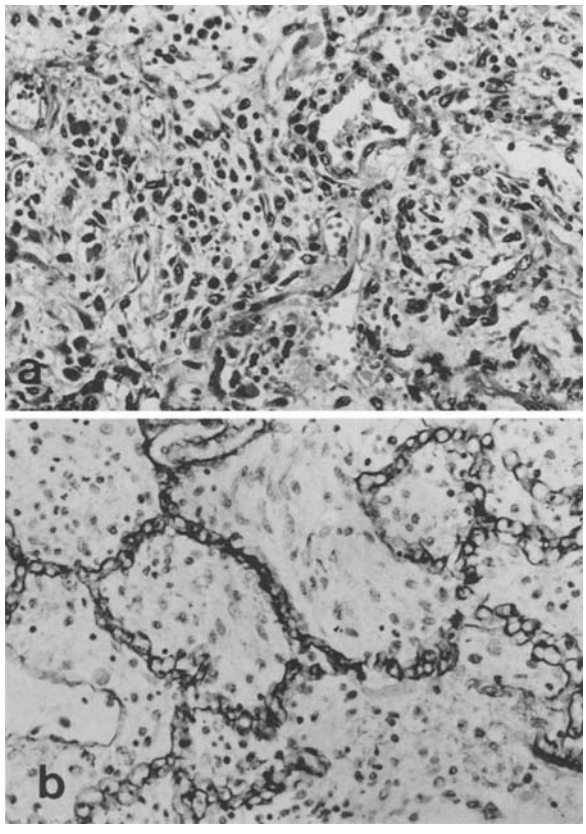

Fig. 9. Case 25. Note complete fibrous obliteration of alveolar spaces with the almost intact basement membrane. These findings are not ascertained in H&E section. (a: H&E, ×170, b: IP-haematoxylin for collagen type IV, ×170)

vessels larger than those of respiratory bronchioles and interlobular septa in the control specimens. No staining was detected in the capillary endothelial cells. Likewise, factor VIII-related antigen was positive in the arterioles and venules in all cases of the paraquat lungs. Alveolar capillaries were also positive in some cases. The original alveolar structures showed immunoreactive cells in the areas of intra-alveolar fibrosis whereas the intraluminal fibrous tissue was devoid of these cells. The findings suggested poor vascularization of the intraluminal fibrous tissue in the paraquat lung. This was in striking contrast to neovascularization of the intraluminal fibrous tissue in the cases of organizing pneumonia (unpublished data).

Vimentin was positive for various mesenchymal cells such as fibroblasts, vascular smooth muscle cells, endothelial cells, and macrophages. In the cases where death occurred within 108 h after ingestion, all interstitial cells except for the vascular smooth muscle cells and endothelial cells were vimentin-negative. On the 7th day and thereafter, vimentin-positive, lysozyme- and alpha-1 antitrypsin-negative polygonal to spindle-shaped cells appeared in the thickened alveolar walls and intraluminal exudate, predominantly near the luminal surface (Fig. 11). On the 20th day, the Masson body contained vimentin-positive cells (Fig. 12).

Immunostaining with anti-desmin antibody clearly delineated smooth muscle cells of the bronchi, vessels, and at the openings of the alveolar ducts. No other cells were positively stained until the 7th day when desmin-positive cells appeared in the thickened alveolar walls. The preexisting smooth muscle cells became hypertrophic on the 13th day. On the 14th day, desmin-positive polygonal to spindle-shaped cells increased in number and became prominent along the luminal surface. There was no close spatial relationship between these cells and the hypertrophic bronchiolar muscle cells (Fig. 13). Some polygonal cells showed a transition to elongated spindle-shaped cells particularly after the 20th day (Fig. 14). On the 24th day, the hypertrophic bronchiolar muscle cells became more prominent. The bronchial lumen was completely obliterated by the fibrous tissue which contained only rare desmin-positive cells (Fig. 15).

In summary, the temporal sequence may be summarized as follows. Congestion, oedema, exudation, and haemorrhage occurred within 20 h after paraquat ingestion. The alveolar epithelium remained intact until 49 h as manifested by a well retained immunoreactivity of EMA. It was after 52 h that the epithelium was damaged. By then, the immunoreactivity of EMA was completely lost. The alveolar and vascular basement membranes marked by collagen type IV antibody were well preserved. Regeneration and organization started focally on the 7th day when the alveolar epithelial basement membrane became clearly separated from the capillary basement membrane. The epithelial basement membrane was now disarrayed and fragmented from place to place. The EMA-positive epithelial cells reappeared on the 8th day. At the same time vimentin-positive polygonal and spindle-shaped cells appeared and gradually increased in number in the course of time. These cells were probably fibroblasts and/or myofibroblasts and located not only in the interstitium but also in the areas of intra-alveolar fibrosis. In the late stage of intra-alveolar fibrosis, the alveolar walls retained the original framework of the basement membrane in some areas. The vimentin-positive mesenchymal cells were present between the newly formed air spaces and the original basement membrane, but were never embedded among the disrupted basement membranes. The epithelial basement membrane was, therefore, considered to

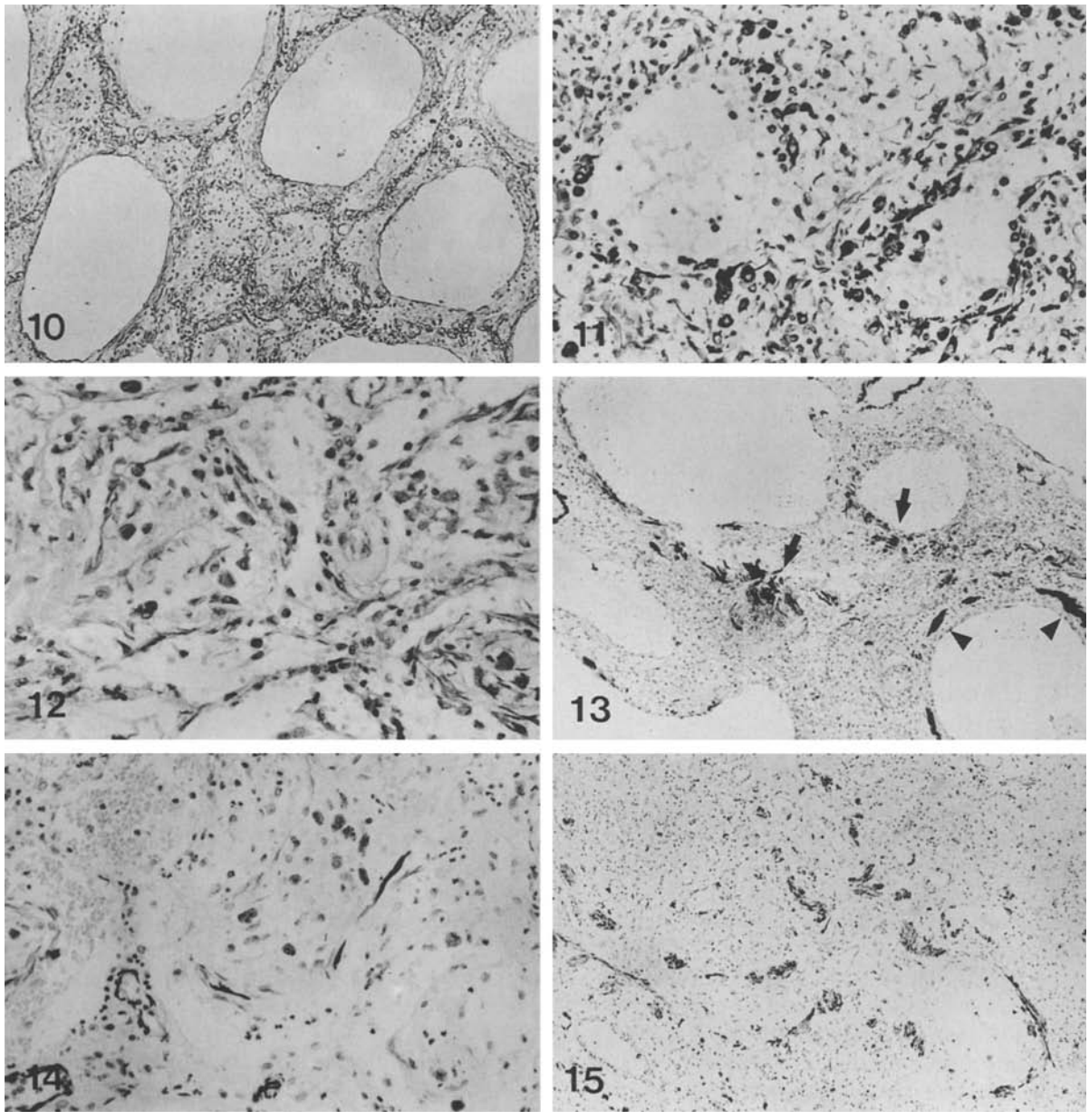

Fig. 10. Case 22. Reaction for collagen type IV shows the original epithelial basement membrane embedded in the thickened interstutium. Fibrous tissue is located on the luminal side of basement membrane. (IP-haematoxylin for collagen type IV, × 60)

Fig. 11. Case 25. Vimentin-positive cells are present predominantly on the luminal surface of intraalveolar fibrosis. (IP-haematoxylin for vimentin, × 150)

Fig. 12. Case 28. Intra-alveolar polypoid fibrous tissue (Masson bodies) contains vimentin-positive cells. (IP-haematoxylin for vimentin, × 180)

Fig. 13. Case 24. There is no close relationship between desmin-positive individual polygonal and/or spindle cells (*arrows*) and hypertrophic muscle cells of bronchioles (*arrowheads*). (IP-haematoxylin for desmin, × 60)

Fig. 14. Case 28. Desmin-positive individual cells are transformed to elongated spindle-shape. (IP-haematoxylin for desmin, × 180)

Fig. 15. Case 29. Note the hyperplastic muscles of the bronchioles totally obliterated with fibrous tissue. Desmin-positive cells are rarely present in the fibrous tissue. (IP-haematoxylin for desmin. × 60)

be only temporally disrupted and repaired within a relatively short period of time. The organization proceeded further and was accompanied by proliferation of EMA-positive epithelial cells and vimentin-positive mesenchymal cells. The newly formed air spaces were lined by epithelial cells in some places and by mesenchymal cells in others. In general, vimentin-positive mesenchymal cells showed a tendency to be distributed on the luminal surface of intraalveolar fibrosis, resulting in further narrowing of the luminal spaces. Smooth muscle cells became hypertrophic on the 13th day and thereafter.

Discussion

Paraquat has toxic effects on various organs such as liver, kidneys, and lungs. It accumulates mainly in the lungs over time and induces pulmonary fibrosis. Biochemical evidence suggests that the damage of the alveolar epithelium is due to the production of superoxide and other free radicals in the presence of paraquat and oxygen (Skillrud and Martin 1984; Smith 1987). The precise pathogenesis of the pulmonary fibrosis is, however, not clear.

In order to elucidate the nature of the fibrosing process in the human paraquat lung, it is essential to identify clearly alveolar epithelium, vascular endothelium, basement membranes, and mesenchymal cells. For this purpose, the immunohistochemical studies were performed in addition to the conventional histological studies of the human paraquat lungs.

The regeneration and repair of the paraquat lung we observed occur in the same sequence as suggested by Martinez-Hernandez (1988). The basement membrane materials are mainly synthesized by the epithelial cells under normal circumstances (Pierce and Nakane 1969). Following lung injury, the alveolar epithelial cells degenerate or become necrotic. The alveoli are filled with an inflammatory exudate. If the alveolar basement membrane is spared, the epithelial cells regenerate along the original framework of the membrane (Hayashi et al. 1975; Katzenstein and Askin 1982a). Experimental work using oleic acid has also shown the same mechanism of regeneration and repair (Vracko 1972). If the alveolar exudate is not lysed, the lesion is organized by granulation tissue with the disruption of the basement membrane and subsequent intra-alveolar fibrosis. This process of fibrosis usually assumes the form of intra-alveolar polypoid fibrosis (Masson body formation). When the alveolar basement membrane is severely damaged by toxic substances or leucocyte induced proteolysis (Mainardi et al. 1980; Campbell et al. 1987), the repair process also results in fibrosis. In this situation, the interstitial mesenchymal cells proliferate and differentiate into fibroblasts and myofibroblasts. These cells migrate through the disrupted basement membrane into the alveolar spaces and secrete extracellular matrix (Fukuda et al. 1985; Fukuda et al. 1987). In addition, the injury to the alveolar epithelium itself may induce fibroblastic proliferation through chemical mediators (Rinaldo and Rogers 1982; Adamson et al. 1988).

Our study revealed that the presence of an intact basement membrane is not essential for re-epithelialization to occur. In the early cases of paraquat intoxication, re-epithelialization takes place on the original intact basement membrane. Whereas in the late stage, the fibrous tissue covers the denuded basement membrane and the regenerating epithelial cells grow over the fibrous tissue. These cells are devoid of the underlying basement membrane and abut directly on the connective tissue. This finding is similar to the electron microscopic findings in neo-epithelialization noted elsewhere (Hayashi et al. 1975).

There are two possible sources of regenerating epithelial cells in the peripheral lung tissue; namely, bronchiolar reserve cells and type II pneumocytes (Kawanami et al. 1982). Type II pneumocytes may originate from or revert to bronchiolar reserve cells (Katzenstein and Askin 1982a; Bowden 1981). This possibility is supported by the fact that the EMA-positive cells were present in some of our cases around the peribronchiolar and subpleural region without transition between the two areas.

On the basis of our present study and of past experience, pulmonary fibrosis can be divided into five types; intraluminal diffuse fibrosis, intraluminal polypoid fibrosis, hyaline membrane incorporation, interstitial fibrosis and atelectatic induration. Basset et al. (1986) reported three morphological patterns of intraalveolar fibrosis; intraluminal buds, which are connected to the alveolar walls by a narrow stalk and partially filled the air spaces, obliterative changes, in which the alveolar spaces are completely obstructed by loose connective tissue, and mural incorporation, which consists of the apposition of broad-based fibrous tissue to the alveolar walls. Their "intraluminal buds" corresponds to our intraluminal polypoid fibrosis and "obliterative changes" to our intraluminal diffuse fibrosis. It should be pointed out that their "mural incorporation" represents an early stage or a mild

form of intraluminal diffuse fibrosis (incomplete obliterative change). Basset et al. (1986) suggested that the obliterative change occurred in the area of severely injured epithelial lining. Diffuse loss of the alveolar basement membrane may not be a prerequisite for the formation of intraluminal diffuse fibrosis. Instead, focal damage to the basement membrane may be sufficient to evoke such fibrosis. However, disruption of the basement membrane may reflect the severity of the alveolar damage, and severity of the exudative changes may determine the severity of ensuing fibrosis. It is of interest to note in our study that the original framework was completely obscured by intra-alveolar fibrosis in the H&E section and yet it was well preserved and clearly delineated in many areas by anti-collagen type IV antibody stain. At any rate, the morphological variants of intraalveolar fibrosis seem to be due not only to the size of the defect of the basement membrane but also to difference in the stage of evolution. Intra-alveolar fibrosis in the paraquat lung is characteristically devoid of blood vessels (Copland et al. 1974). We do not have any explanation of the mechanism of this process, but the fibroblastic proliferation is cleary not accompanied by neovascularization. The collapse and coalescence of the alveolar spaces with distention of the alveolar ducts, probably as a result of loss of epithelial cells and surfactant, result in additional fibrosis due to atelectatic induration (Basset et al. 1986). This is a mechanism comparable to the pathogenesis of idiopathic pulmonary fibrosis (Katzenstein 1985) and a similar process is operative in the remodelling of the alveolar structures in the human paraquat lung.

In summary, the morphological changes in the paraquat lung progress in the following way.

Disintegration of the alveolar epithelium develops first with denudation of the underlying basement membranes, the epithelial basement membrane becomes irregular, fragmented and disappears focally. At the same time, the interstitial mesenchymal cells are activated and migrate into the alveolar spaces where they continue to proliferate. Thickening of the alveolar walls and obstruction of the alveolar spaces by fibrous tissue ensue and regeneration of the epithelial cells occurs along the basement membrane in the early stage and directly on the fibrous tissue later. Interstitial, and various types of intraalveolar fibrosis occur in the course of time.

Acknowledgements. The authors would like to thank Dr. Takuya Moriya. Department of Human Pathology, Kawasaki Medical School, for his help in obtaining paraquat lung tissues, and Prof. Toshiharu Matsushima, Department of Medicine, Kawasaki Medical School, for assistance and support throughout this project.

References

Adamson IYR, Young L, Bowden DH (1988) Relationship of alveolar epithelial injury and repair to the induction of pulmonary fibrosis. Am J Pathol 130:377–383

Basset F, Lacronique J, Ferrans VJ, Fukuda Y, Crystal RG (1984) Intraalveolar fibrosis: A second form of fibrosis of the interstitial lung disorders (Abstr). Am Rev Respir Dis 129 (Part II):A-72

Basset F, Ferrans VJ, Soler P, Takemura T, Fukuda Y, Crystal RG (1986) Intraluminal fibrosis in interstitial lung disorders. Am J Pathol 122:443–461

Bowden DH (1981) Alveolar response to injury. Thorax 36:801–804

Campbell EJ, Senior RM, Welgus HG (1987) Extracellular matrix injury during lung inflammation. Chest 92:161–167

Chen K, Demetris AJ, VanThiel DH, Whiteside TL (1987) Double immunoenzyme staining method for analysis of tissue and blood lymphocyte subsets with monoclonal antibodies. Lab Invest 56:114–119

Copland GM, Kolin A, Shulman HS (1974) Fatal pulmonary intra-alveolar fibrosis after paraquat ingestion. N Engl J Med 291:290–292

Dearden LC, Fairshter RD, McRae DM, Smith WR, Glauser FL, Wilson AF (1978) Pulmonary ultrastructure of the late aspects of human paraquat poisoning. Am J Pathol 93:667–680

Fukuda Y, Ferrans VJ, Schoenberger CI, Rennard SI, Crystal RG (1985) Patterns of pulmonary structural remodeling after experimental paraquat toxicity: The morphogenesis of intraalveolar fibrosis. Am J Pathol 118:452–475

Fukuda Y, Ishizaki M, Masuda Y, Kimura G, Kawanami O, Masugi Y (1987) The role of intraalveolar fibrosis in the process of pulmonary structural remodeling in patients with diffuse alveolar damage. Am J Pathol 126:171–182

Greenberg DB, Reiser KM, Last JA (1978) Correlation of biochemical and morphologic manifestations of acute pulmonary fibrosis in rats administered paraquat. Chest 74:421–425

Hara H, Moriya T, Manabe T (1988) Immunohistochemical study of alveolar epithelium in paraquat poisoning. Jpn J Thorac Dis 26:499–506 (in Japanese with English abstract)

Hayashi T, Palpa B, Stemmermann GN (1975) Gastric organ culture: A model for reepithelialization. Am J Pathol (1975) 78:23–32

Huang S, Minassian H, More JD (1976) Application of immunofluorescent staining on paraffin sections improved by trypsin digestion. Lab Invest 35:383–390

Katzenstein AA (1985) Pathogenesis of "fibrosis" in interstitial pneumonia: An electron microscopic study. Hum Pathol 16:1015–1024

Katzenstein AA, Askin FB (1982a) Diffuse alveolar damage. In: Katzenstein AA, Askin FB (eds) Major Problems in Pathology, vol 13. Surgical pathology of non-neoplastic lung disease. WB Saunders Company, Philadelphia, pp 9–42

Katzenstein AA, Askin FB (1982b) Chronic interstitial pneumonia, interstitial fibrosis, and honeycomb lung. In: Katzenstein AA, Askin FB (eds) Major Problems in Pathology, vol 13. Surgical pathology of non-neoplastic lung disease. W.B. Saunders Company, Philadelphia, pp 43–72

Kawanami O, Ferrans VJ, Crystal RG (1982) Structure of alveolar epithelial cells in patients with fibrotic lung disorders. Lab Invest 46:39–53

Mainardi CL, Dixit SN, Kang AH (1980) Degradation of type IV (basement membrane) collagen by a proteinase isolated from human polymorphonuclear leukocyte granules. J Biol Chem 255:5435–5441

Martinez-Hernandez A (1988) Repair, regeneration, and fibrosis. In: Rubin E, Farber JL (eds) Pathology. JB Lippincott Company, New York, pp 66–95

McGovern J, Crocker J (1986) Effect of formalin pigment removal on peroxidase-antiperoxidase immunoperoxidase technique. J Clin Pathol 39:923–926

Moriya T, Hara H, Manabe T (1988) Intra-alveolar fibrosis in the paraquat lung: A histological analysis of 29 autopsy cases. Kokyu 7:359–365 (in Japanese with English abstract)

Mukada T, Sasano N, Sato K (1978) Autopsy findings in a case of acute paraquat poisoning with extensive cerebral purpura. Tohoku J Exp Med 125:253–263

Ordónẽz NG, Manning JT Jr, Brooks TE (1988) Effect of trypsinization on the immunostaining of formalin-fixed, paraffin-embedded tissues. Am J Surg Pathol 12:121–129

Parkinson C (1980) The changing pattern of paraquat poisoning in man. Histopathology 4:171–183

Pierce GB, Nakane PK (1969) Basement membranes: Synthesis and deposition in response to cellular injury. Lab Invest 21:27–41

Rebello G, Mason JK (1978) Pulmonary histological appearances in fatal paraquat poisoning. Histopathology 2:53–66

Rinaldo JE, Rogers RM (1982) Adult respiratory-distress syndrome: Changing concepts of lung injury and repair. N Engl J Med 306:900–909

Schoenberger CI, Rennard SI, Bitterman PB, Fukuda Y, Ferrans VJ, Crystal RG (1984) Paraquat-induced pulmonary fibrosis. Am Rev Respir Dis 129:168–173

Skillrud DM, Martin WJ II (1984) Paraquat-induced injury of type II alveolar cells: An in vitro model of oxidant injury. Am Rev Respir Dis 129:995–999

Smith LL (1987) Mechanism of paraquat toxicity in lung and its relevance to treatment. Hum Toxicol 6:31–36

Smith P, Heath D (1973) The ultrastructure and time sequence of the early stages of paraquat lung in rats. J Pathol 114:177–190

Spencer H (1985) Paraquat lung. In: Spencer H (ed) Pathology of the lung, 4th ed. Pergamon press, Oxford, pp 719–721

Sternberger LA, Hardy PH Jr, Cuculis JJ, Meyer HG (1970) The unlabeled antibody-enzyme method of immunohistochemistry: Preparation and properties of soluble antigen-antibody complex (horseradish peroxidase-antihorseradish peroxidase) and its use in identification of spirochetes. J Histochem Cytochem 18:315–333

Sykes BI, Purchase IFH, Smith LL (1977) Pulmonary ultrastructure after oral and intravenous dosage of paraquat to rats. J Pathol 121:233–247

Thurlbeck WM, Thurlbeck SM (1976) Pulmonary effects of paraquat poisoning. Chest 69:276–280

Vracko R (1972) Significance of basal lamina for regeneration of injured lung. Virchows Arch [A] 355:264–274

Yamaguchi M, Takahashi T, Togashi H, Arai H, Motomiya M (1986) The corrected collagen content in paraquat lungs. Chest 90:251–257

Received February 11, 1989 / Accepted April 24, 1989